10. B. E. Launder, C. H. Priddin, and B. I. Sharma, "The calculation of turbulent boundary layers on spinning and curved surfaces," Trans. ASME, J. Basic Eng., 99, No. 1 (1977).
11. A. A. Samarskii, Theory of Difference Methods [in Russian], Nauka, Moscow (1977).
12. K. K. Fedyaevskii, A. S. Ginevskii, and A. V. Kolesnikov, Computation of Incompressible Turbulent Boundary Layer [in Russian], Sudostroenie, Leningrad (1973).
13. O. N. Ovchinnikov and E. M. Smirnov, "Dynamics of flow and heat transfer in rotating slot-type channel," Inzh. Fiz. Zh., 35, No. 1 (1978).
14. K.-Y. Chien, "Predictions of channel and boundary-layer flows with a low-Reynolds-number turbulence model," AIAA J., 20, No. 1 (1982).
15. Kh. Greenspan, Theory of Rotating Fluids [in Russian], Gidrometeoizdat, Leningrad (1975).

FLOW OVER LAMBDA WINGS WITH FLAPS

O. N. Ivanov and A. I. Shvets

UDC 533.6.011.55+629.782.015.3

Flow over wings of lambda-shaped cross section and over star-shaped bodies has been investigated in [1-5].

For control of an aircraft in the cruise regime and also for takeoff and landing one must have mechanical devices such as flaps. Their effectiveness depends considerably on boundary layer separation. Separation on two-dimensional and axisymmetric bodies, and also three-dimensional separation in flow over obstacles have been studied in a number of papers, but as yet limited data are available on boundary layer separation on triangular wings with flaps [6]. No data have as yet been published on lambda wings with flaps.

The flow and boundary layer separation on lambda-shaped wings with flaps have been investigated in a supersonic wind tunnel at $M = 0.3$-3 and $Re_c = (1\text{-}3)\cdot 10^6$. We tested three models of triangular lambda wings with vertex angles $\Lambda = 180$, 160, 121° and sweepback angle in the wing plane of $\chi = 71°$ (Fig. 1). For all three models the flap slope angle was $\delta = 0$ and 40°, and for the model with vertex angle $\Lambda = 161°$ we also tested at $\delta = 21°$. The wing span for all three models was $R = 140$ mm, and the thickness was 10 mm. The wing leading edges were made sharp, with a wedge angle of $\beta = 25°$, to obtain an attached shock wave at $M = 3$. The models were attached to the α-mechanism by means of a rear sting with $d = 28$ mm and $l = 200$ mm, in the form of a half cylinder with a wedge cutaway ($\psi = 20°$) along the central chord of the leeward side of the lambda wing. The pressure at points on the model surface with coordinates s along the central chord $c = 200$ mm was measured with an induction sensor, with the aid of a pressure commutator. The relative error of pressure measurement was ±2%. The oil film method was used to investigate the stream lines and the separation boundaries on the surface of the wing and the flap.

We shall examine the influence of the vertex angle Λ (Fig. 1a, $\alpha = 15°$, $M = 3$, $\delta = 40°$, points 1-3 refer to $\Lambda = 180$, 161, 120°) and the flap deflection angle δ (Fig. 1b, $\alpha = 15°$, $M = 3$, $\Lambda = 161°$, points 4-6 refer to $\delta = 0$, 21, 40°) on the pressure distribution and the location of the separation point. The pressure distribution curves on the lambda wings and in the plane of the triangular wing ($\Lambda = 180°$) are similar, while the pressure on the flap continues to increase as the angle Λ is reduced. It was established from the pressure measurements of [6] that the nature of the pressure distribution changes very little over the span of a plane triangular wing, in spite of the flow being three-dimensional in this zone. However, the pressure on the flap varies appreciably over its span because of the intense spreading of the flow, and the maximum pressure is found in the central part. The vertex angle $\Lambda = 161°$ is close to the optimal angle of $\Lambda = 150°$ to certain the maximum lift-to-drag ratio in the class of equivalent wings [4]. On this lambda wing model we studied the flow for three values of the flap deflection angle ($\delta = 0$, 21, 40°) (see Fig. 1b). The flap deflection at angle $\delta = 21°$ for $\alpha = 0$ gives a sharp pressure increase only on the flap, and at $\alpha = 15°$ in the immediate vicinity of the wing-flap discontinuity ($s/c = -0.025$) (see Fig. 1b), which agrees with the results of [6], where nonseparated flow was found at hypersonic speeds for a plane triangular wing with flap deflection angles $\delta \leqslant 20°$. In addition, for this flap we

Moscow. Translated from Zhurnal Prikladnoi Mekhaniki i Tekhnicheskoi Fiziki, No. 5, pp. 41-46, September-October, 1985. Original article submitted June 15, 1984.

 0021-8944/85/2605-0640$09.50

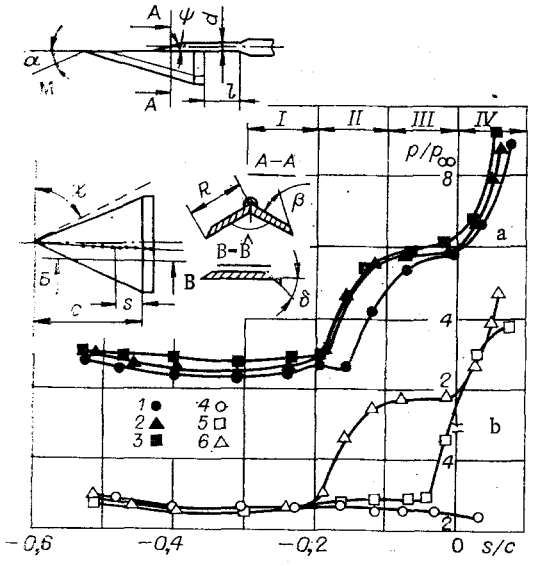

Fig. 1

find a "pressure plateau" in the separated zone, and the pressure equilibration at the trailing edge is evidence that the reduced pressure behind the flap is transmitted upstream along the boundary layer and on the flap.

For a flap deflection of $\delta = 40°$ the separated zone is propagated energetically upstream (see Fig. 1b). An increase in the angle of attack causes a pressure increase in the separated zone ($s/c = 0.15$), and, in contrast with the case of $\delta = 21°$, the pressure in the separation zone becomes almost constant. The graph of the pressure distribution at large flap deflection angle ($\delta = 40°$) can be divided into four zones (see Fig. 1): I) nonseparated flow ($s_I/c = -1$–-0.2); II) the start of boundary layer separation ($s_{II}/c = -0.2$–-0.1), characterized by a pressure increase; III= separated flow ($s_{III}/c = -0.1$–0) with a small pressure gradient; and IV) flow on the flap ($s_{IV}/c = 0$–0.1) with a strong pressure increase.

It is known that the width of the separation zone on a triangular wing depends on a whole series of parameters: the Mach number, the flap deflection angle, the flap height (if this is comparable with the boundary layer thickness), and the temperature factor of the suction intensity. An additional factor appears in investigations of lambda wings: the vertex angle of the lambda wing, where the confinement of transverse flow spreading plays an appreciable role. The location of the separation point for a lambda wing with $\Lambda = 161°$ is found to be closer to the model nose than for a flat wing ($\Lambda = 180°$) (see Fig. 1a). Because of the pressure transmission mechanism the separation point moves upstream until a pressure gradient forms in the boundary layer, leading to an equilibrium of inertia, friction and pressure forces in the region of the separation point. The displacement of the separation point upstream on a lambda wing expands the separation zone, which also expands the section of increased presure, and therefore the pressure drag and the total drag increase. However, further progression of wings from $\Lambda = 161°$ to $\Lambda = 120°$ has practically no influence on the width of the separation zone along the chord.

Figure 2 shows a suggested flow scheme, constructed from the results of investigations using a carbon black–oil coating and flow photographs: 1) the laminar boundary layer; 2) the turbulent boundary layer; 3) the separation boundary; 4) the trailing edge circulation flow; 5) the central vortex region; 6) the shock on the wing; 7) the shock ahead of the separation zone; and 8) the shock ahead of the flap. Inside the separation zone near the triangular surface of the lambda wing two vortices 5 are formed (Fig. 2a). The vortices detach from the main flow and move close to the flap surface. Formation of vortices in the central regions leads to a vigorous removal of the gas from this zone. Therefore, along with the formation of a "mixed" separation zone one finds that the separation point in the middle part of a lambda wing is displaced downstream. A "mixed" separation zone can be formed in the turbulent boundary layer case near the central chord, and near the edge for a laminar or transitional boundary layer. Near the wing-flap junction line additional vortex regions 4 form on the wing surface, and these have been recorded in the form of oil–black concentrations. A decrease of the vertex angle Λ leads to an increase of the trailing edge vortices. An added

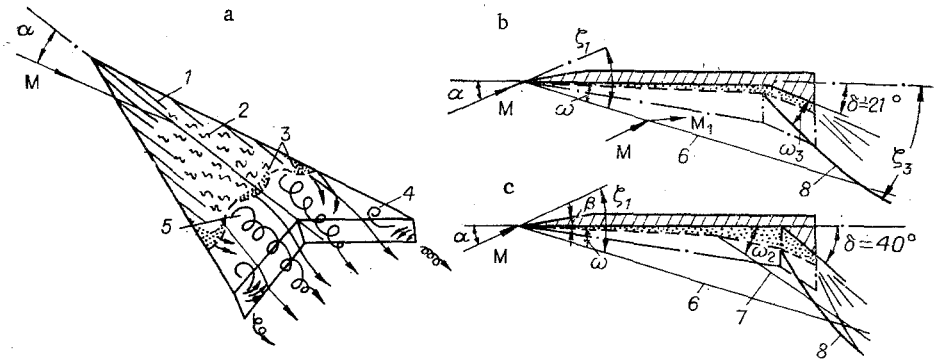

Fig. 2

series of experiments was conducted to study the influence of flaps on the trailing edge vortex regions. In these tests the ends of the flaps were cut off at an angle of 30°, and this led to a compression of the separation zone, reduced strength of the trailing vortices and increased transverse overflow across the edges near the flaps.

We now consider change of shock wave shape in the wing symmetry plane (Fig. 3). In supersonic flow over a lambda wing at M = 3 at zero angle of attack a perturbation wave forms ($\mu = 19.4°$) which begins from the wing vertex. With increase of angle of attack the flow is deflected from the initial direction and a bow shock is formed ahead of the model, located at angle ζ_1 to the incident stream velocity vector (the shock slope angle), and at angle ω to the axis of the lambda wing model (see Fig. 2b). The relation between the angle ζ_1, the angle ω, and the angle of attack α can be expressed by the relation $\zeta_1 = \omega + \alpha$. In the case of flow over triangular wings and over lambda wings with flaps mounted at angle $\delta = 21°$ the flow remains unseparated. On the flap there is additional flow deflection with formation of a shock wave. The structure of the shock waves in Fig. 2b illustrates unseparated supersonic flow on the flap, when the flow deflection angle $\alpha + \delta$ and the shock wave slope angle ζ_3 are less than the critical value (for a wedge at M = 3 the critical flow deflection angle is $\delta_* = 32°$, and the shock wave slope angle is $\zeta_* = 66°$).

The slope angle of the bow shock from the model nose ζ_1 is shown in Fig. 3 ($\Lambda = 161°$, $\delta = 21°$, M = 3) as a function of the angle of attack. For comparison with the data for lambda wings Fig. 3 shows the dependence of the shock slope angle on the half angle at a wedge vertex and on the half angle at a cone vertex θ, and compares the experimental data on the shock angles ζ_3 on the flap with the shock slope angle ζ for a wedge (broken lines) and a cone (dot–dash lines) with a vertex half angle equal to the flap deflection angle ($\theta = \delta = 21°$). Here the Mach numbers of the flow over the wedge and cone were found from the value of M_1 behind a plane shock corresponding to flow deflection at the wing angle of attack (for angle of attack $\alpha = 5$, 10, and 15°, $M_1 = 275$, 2.5, and 2.25). The shock slope angles ζ_1 and ζ_3 for the wings fall in the region bounded by the shock slope angles for the cone and the wedge. The shock slope angle ζ_3 for a deflected wing at angle $\delta = 21°$ does not reach the critical value for an increase of the angle of attack α up to 10°. In this case no boundary-layer separation was observed in the investigation using the oil–black coating method. For $\alpha = 15°$ on the lambda wing surface we saw the separation boundary immediately ahead of the flap, which corresponds to a sharp pressure increase (see Fig. 1b). A flap deflection at angle $\delta = 40°$ causes flow separation and a system of shocks, with expansion of the separation zone as the angle of attack increases (see Fig. 2c). For the wings tested the bow shock (the shock 6) in the plane of symmetry is a straight line over most of the chord, and a second shock 7 forms at the separation point. Ahead of the flap there is a shock 8 with a curved front, due to flow deflection by an angle larger than critical ($\delta = 40°$) for the corresponding flow regime, and subsonic flow is found on the flap. With increasing distance downstream from the flap axis the shock slope angle ζ_3 decreases (see Fig. 2b), and over a certain section remains larger than the value corresponding to subsonic flow. Further downstream the shock slope ζ_3 tends to a value corresponding to a perturbation wave, $\zeta_3 = \mu = \arcsin(1/M)$.

For transonic and subsonic flow over lambda wings without flaps ($\delta = 0$) and with flaps at angle of attack $\alpha = 15°$ (Fig. 4) the pressure in the base region decreases. This is associated with the effect of transmission of reduced pressure in the near wake to the flap. As for supersonic flow, the windward surface pressure has a tendency to increase with reduced vertex angle. The combination of a lambda wing with a flap gives a qualitatively

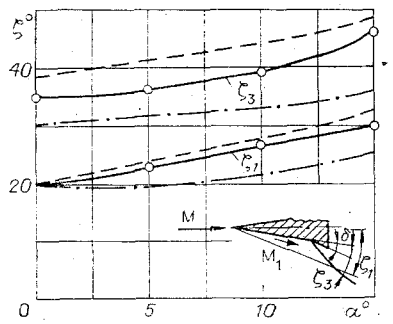

Fig. 3

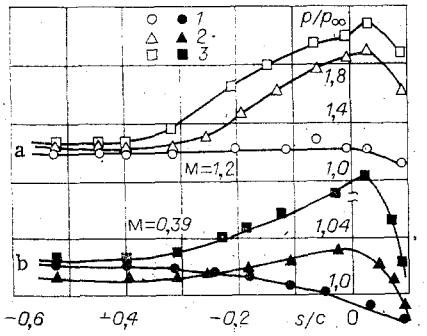

Fig. 4

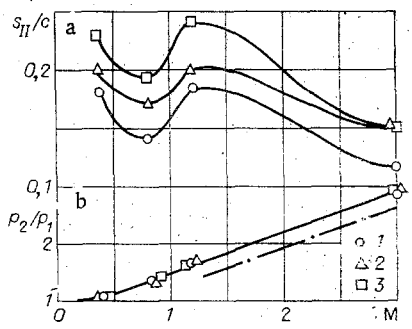

Fig. 5

different flow picture at M = 1, 2 than at M = 3. For example, for M = 1, 2 the increased pressure zone expands appreciably and reaches the point s/c = −0.45 (Fig. 4a, $\Lambda = 161°$, M = 1, 2, $\alpha = 15°$, points 1-3 correspond to $\delta = 0, 21, 40°$, respectively). In this zone there is no clearly pronounced "pressure plateau," the pressure on the flap reaches a maximum and decreases near the trailing edge, and one also finds regimes for which the pressure is decreased over the entire flap chord. The expansion of the separated flow region due to the proximity of the wings appears at all angles of attack more strongly than for M = 3.

The pressure ahead of the flap at subsonic speed (M = 0.39), as for M = 1, 2, increases smoothly and reaches its maximum in the flap region (Fig. 4b). With increase in the vertex angle the concavity of the pressure curve is reduced, which is evidence of overflow on the leeward side of the lambda wing, and the volume of the separated zone decreases because the vortices come close to the surfaces. We note that the influence of incident flow velocity on the pressure distribution is much more appreciable than the influence of the vertex angle. While for flow over a lambda wing at velocity corresponding to M = 1, 2 with increase of flap deflection ($\delta = 0, 21, 40°$) we observe a considerable pressure increase over the wing chord (see Fig. 4a), for low Mach numbers (M = 0.39) the influence of angle of attack and flap deflection angle is very little (see Fig. 4b). In this case the influence of the base region and the leeward side of the model extends over the whole flap.

One should note the influence on the increased pressure zone of Mach number variation (Fig. 5a, $\delta = 40°$, $\alpha = 15°$, points 1-3 correspond to $\Lambda = 180, 161, 120°$, respectively). With increase of M the distribution of the aerodynamic pressure over the wing changes, and in the transonic flow range an expansion of the increased pressure region s_{II}/c causes an increased pressure drag. A similar variation of the increased pressure zone (Fig. 5a) in the transonic region can cause sharp changes in the location of the center of pressure and can influence the stability and control of the aircraft.

For all the flow separation cases the pressure p_1 increases and reaches some constant value p_2 in the separated zone (the so-called separation zone plateau). The parameter p_2/p_1 is called the critical pressure ratio in the oblique shock arising ahead of the separation point. The critical pressure ratio does not depend on the method of generating the shock, but is only a function of the Mach number (Fig. 5b, dot-dash line, $\delta = 40$, $\alpha = 0$) and is approximated by a formula of the form [7]

$$p_2/p_1 = 0.515 + 0.675\ \mathrm{M}.$$

With increase of M the critical pressure ratio increases, and the vertex angle Λ has a slight influence on the value p_2/p_1, while a decrease of Λ causes an expansion of the increased pressure zone s_{II}/c (see Fig. 5a).

LITERATURE CITED

1. T. R. P. Nonweiler, "Aerodynamic problems of manned space vehicles," J. Roy. Aeron. Soc., 63, 521 (1959).
2. G. I. Maikapar, "The wave drag of nonaxisymmetric bodies in supersonic flow," Prikl. Mat. Mekh., 23, No. 2 (1959).
3. G. F. Chernyi and A. L. Gonor, "The determination of body shapes of minimum drag using the Newton and Busemann pressure laws," Paper at the Symp. on Extremal Problems in Aerodynamics, Washington, Boeing Sci. Res. Labs., Seattle (1962).
4. A. L. Gonor and A. I. Shvets, "Flow over V-shaped wings at M = 4," Izv. Akad. Nauk SSSR, Mekh. Zhidk. Gaza, No. 6 (1967).

5. V. A. Vordyug, Yu. A. Vedernikov, et al., "Parametric investigation of hypersonic three-dimensional shapes," Zh. Prikl. Mekh. Tekh. Fiz., No. 1 (1983).
6. M. L. Whitehead and Kies, "Flow picture and separation on triangular wings with flaps at M = 6," Raketn. Tekhn. Kosmonavt., 6, No. 12 (1968).
7. Yu. A. Panov and A. I. Shvets, "Separation of a turbulent boundary layer in supersonic flow," Prikl. Mekh., 2, Issue 1 (1966).

DETERMINATION OF THE INTENSITY OF A FREE VORTEX SHEET WITHIN THE FRAMEWORK OF LIFTING SURFACE THEORY

N. F. Vorob'ev

UDC 533.69

A free vortex sheet leaving the edge of a small-span wing exerts substantial influence on its lifting properties. The problem of the flow around a finite span wing is a potential stream reduces in lifting surface theory to singular integrodifferential equations with a free surface. The method of discrete vortices turns out to be effective for the solution of problems on the flow around a wing with a free surface. A discrete vortex scheme is proposed in [1] for a finite span thin wing in which the intensity of the vortex line congruent with the wing leading (including side) edge is assumed equal to the intensity of an attached line vortex that goes over into a free vortex on the wing independently of the wing planform. However, as comparison between the numerical computations performed [2] and experimental results shows, the intensity of a free vortex sheet, exactly as its configuration, depends on the wing planform and the degree of wing roundoff and deflection. In the case of thin wings with plane middle surface, the principal factor governing the convergent vortex sheet is the wing planform. A discrete vortex sheet is proposed in [2-4] for a finite-span wing, where the dependence of the intensity of the free vortex sheet on the wing geometry is taken into account by the introduction of a parameter $0 \leqslant K \leqslant 1$. The value $K = 0$ on the wing corresponds to the regime of unseparated flow around a wing, and $K = 1$ to the model used in [1]. The magnitude of the parameter $0 \leqslant K \leqslant 1$ for a specific sweep angle was established by comparing computed and experimental results.

Convergent conditions for finite-span wings are formulated in this paper that permit determination of the dependence of the free vortex sheet on the local wing sweep angle in explicit form by starting from the line vortex conservation conditions in a potential flow. Results of a computation of the total aerodynamic characteristics of rectangular and triangular wings of different spans are compared with existing experimental data obtained in wind tunnels.

In conformity with vortical lifting surface theory, the vortex surface attached to the wing trailing edge goes smoothly over into a free vortex surface; the line vortex intensity is here conserved. On the wing leading (side) edges, the nature of the runoff of the vortical layers from the lifting surface is determined by their interaction with the free stream. According to available experiments on bubble visualization in flow channels and oil—soot visualization of streamline tracks on wing surfaces in a wind tunnel, the streamline (line vortex) pattern in the flow over a triangular thin plate at an angle of attack is shown schematically in Fig. 1a, where the free vortex surface convergent with the leading edge is displayed on the left side of the wing, and streamlines on the upper wing surface, on the right. The leading edge is the envelope of surface stream lines approaching the wing and the line vortices convergent with the wing. The attached line vortex (vortex tube) is divided into two components upon approaching the edge L and touching it; a line that has a direction in agreement with the tangent to the wing edge, and remains connected to the wing and a line that converges with the wing surface while becoming a free line vortex (Fig. 1b). The binormal velocity component from the free stream side hinders runoff of the thin vortical layers at the leading edge. As numerous experiments show, the intensity of the vortex sheet coincident with the leading edge in thin wings around which there is flow at an angle of attack will grow as the sweep angle of the edge increases.

Novosibirsk. Translated from Zhurnal Prikladnoi Mekhaniki i Tekhnicheskoi Fiziki, No. 5, pp. 46-50, September-October, 1985. Original article submitted November 30, 1984.

 0021-8944/85/2605-0644$09.50